

### 3. LIGHT SOURCE

#### 3.1 Introduction

The Photon Factory manages two light sources: the 2.5 GeV PF ring and the 6.5 GeV PF-AR. The principal beam parameters for the two storage rings are given in Table 1, and spectra from the various insertion devices and bending magnets of the two rings are summarized in Fig. 1.

Since its first commissioning in 1982, the PF ring has been upgraded twice in 1986 and 1997 in order to reduce the beam emittance from 450 nm rad to 36 nm rad. In 2005, we completed a third major upgrade project to produce new short straight-sections and to extend existing straight sections in order to satisfy increasing demands for various types of new insertion devices. The operation status of the PF ring is reported in section 3.2, the straight-sections upgrade will be described in section 3.3, and future plans for top-up injection will be briefly reported on in section 3.4.

The PF-AR was originally constructed as a booster synchrotron for the TRISTAN main ring. After the expiration of the TRISTAN project, it was converted to a dedicated synchrotron radiation source. The beam ducts of the PF-AR were completely replaced in 2001 in order to improve the vacuum system and its stability as a light source. Parallel to the ring upgrade, a new experimental hall building was constructed in the north-west area. The stored beam lifetime of the PF-AR has been dramatically improved through the successful completion of the reconstruction. The operation status of the PF-AR will be described in section 3.5.

After 2001, the construction of new undulator beamlines was continued both in the new experimental hall of the PF-AR and in the straight sections of the PF ring. Various types of undulators have been installed for

these new beamlines, and the development of these will be described in section 3.6.

#### 3.2 Operation Status of the 2.5 GeV PF Ring

The complete operation time history for the PF ring is shown in Fig. 2. In 1997, there was a half-year shutdown for reconstruction in order to reduce the beam emittance. This was carried out by replacing old quadrupole and sextupole magnets in the arc sections. Following this reconstruction the total operation time was increased and maintained at around 5000 hours per year. A further half-year shutdown took place in 2006 for the straight-sections upgrade project. Details of this upgrade will be described in the next section.

In FY2004, the scheduled user time was 4080 hours, and the actual user time excluding time losses due to machine trouble and daily injections was 3999 hours. The ratio of actual user time to scheduled time has been maintained at 96-98% over the past 5 years. Most of the user time is operated under 2.5-GeV multi-bunch mode. About 10% of user time is assigned for 3-GeV multi-bunch operation and another 10% for 2.5-GeV single-bunch operation every year.

Figure 3 shows the trend of the product  $I\tau$  of the beam current  $I$  and the beam lifetime  $\tau$  after the emittance upgrade in 1997, and Fig. 4 shows the history of the average stored current since 1982. Although the initial beam current has been maintained at a constant 450 mA for several years, a gradual increase in average beam current corresponding to an increase in the  $I\tau$  product is noticeable. After low-emittance operations started in 1998, the limitation of the beam lifetime due to the Touschek effect became very serious. The estimated Touschek lifetime under multi-bunch operation was comparable to, or shorter than, the beam-gas scattering

Table 1 Principal beam parameters of the PF Ring and PF-AR.

	PF	PF-AR
Energy	2.5 GeV (3 GeV)	6.5 GeV (5 GeV*)
Natural emittance	36 nm rad	293 nm rad
Circumference	187 m	377 m
RF frequency	500.1 MHz	508.6 MHz
Bending radius	8.66 m	23.2 m
Energy loss per turn	0.4 MeV	6.66 MeV
Damping time		
Vertical	7.8 ms	2.5 ms
Longitudinal	3.9 ms	1.2 ms
Natural bunch length	10 mm	18.6 mm
Momentum compaction factor	0.0061	0.0129
Natural chromaticity		
Horizontal	-12.5	-14.3
Vertical	-12.3	-13.1
Stored current	450 mA	60 mA (70 mA*)
Number of bunches	280	1(2*)
Beam lifetime	60-80 hr (at 450 mA)	12 hr (at 60 mA)

\* Double bunch operation at 5 GeV for medical applications

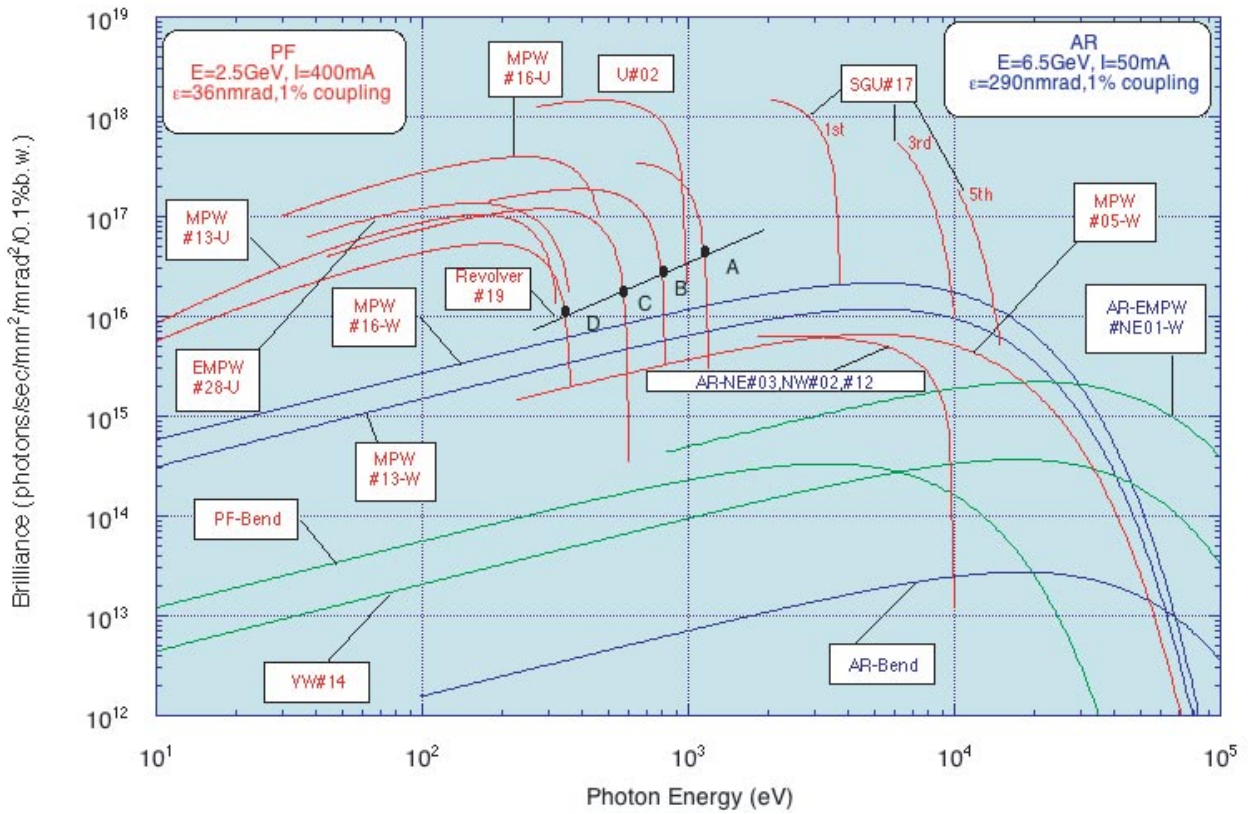


Figure 1  
 Synchrotron radiation spectra available at the PF Storage Ring (2.5 GeV) and the PF-AR (6.5 GeV). Brilliance of radiation vs. photon energy for the insertion devices (U#02, MPW#05, MPW#13, VW#14, SGU#17, MPW#16, Revolver#19 and EMPW#28) and the bending magnet (PF-Bend) of the PF Storage Ring, and for the insertion devices (EMPW#NE1, U#NE03, U#NW02 and U#NW12) and the bending magnet (AR-Bend) of the PF-AR. Several insertion devices have both undulator and wiggler modes, which are denoted by U and W, respectively (the undulator mode of AR-EMPW#NE01 is not shown). The spectral curve of each undulator (or undulator mode of multipole wiggler) is a locus of the peak of the first harmonic within the allowance range of K-parameter. Spectra of Revolver#19 are shown for four kinds of period. Please note that not the first harmonic but the third or fifth harmonic is used for X-ray experiments at BL-17, AR-NE3, AR-NW2 and AR-NW12 beamlines.

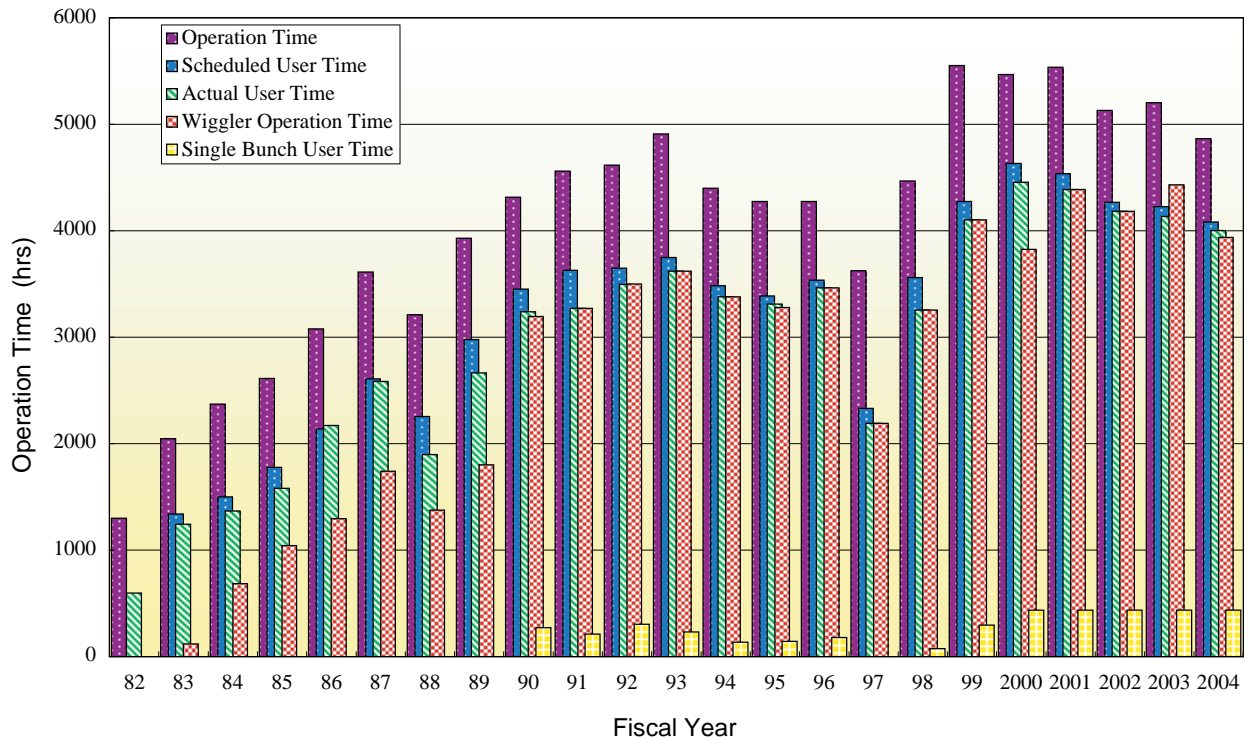


Figure 2  
 Operation time history of the PF Storage Ring.

lifetime. In order to improve this situation, we modulated the RF phase at a frequency of twice the synchrotron frequency, and induced a longitudinal quadrupole-mode oscillation of the bunches. Using this method, the lifetime was improved by a factor of about two. Thanks to the very long lifetime of over 60 hours (at 450 mA), the

beam is now injected only once a day and the beam current is maintained above 330 mA between injections.

The change in the failure rate, defined as the ratio of failure time to the total operation time, is shown in Fig. 5. The failure rate has been maintained at around 1% over the past 10 years, and about 0.5% over the past 3

Table 2 Causes of unscheduled beam dumps at the PF ring during user operation in 2003.

causes of beam dump	number of beam dumps
RF system failure	4
earthquake	2
user misoperation (unintended dump)	3
magnet power-supply failure	1
<b>total number of beam dumps</b>	<b>10</b>

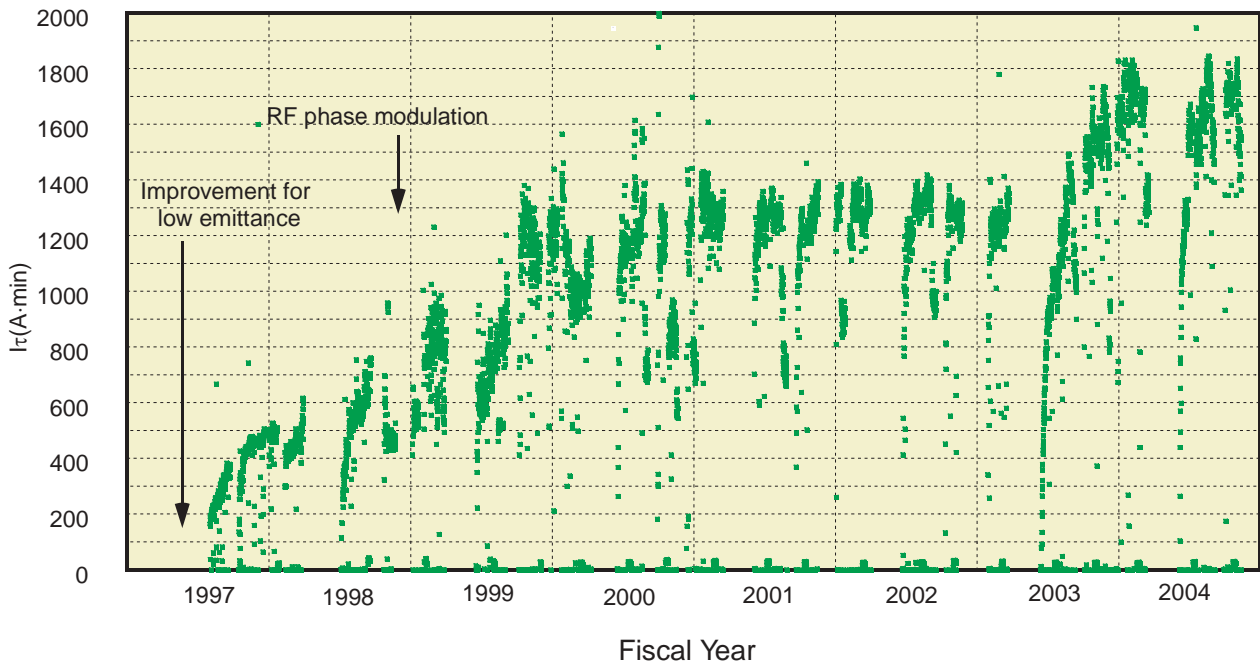


Figure 3  $I\tau$  history of the PF Storage Ring over the past 8 years.

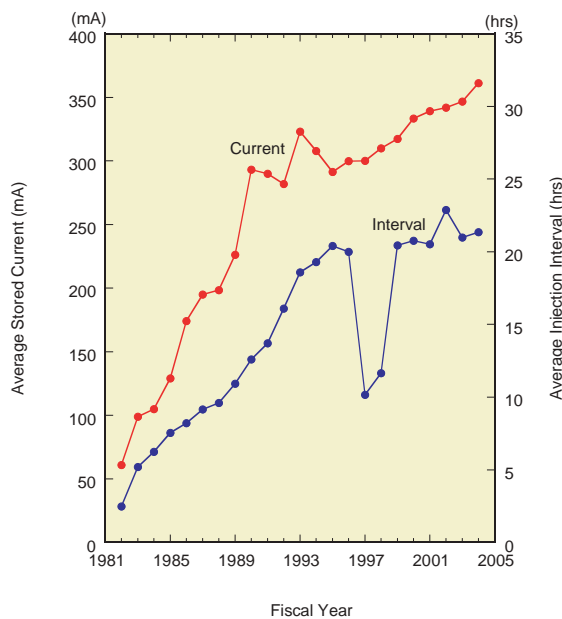


Figure 4 Average stored current and injection interval since 1982.

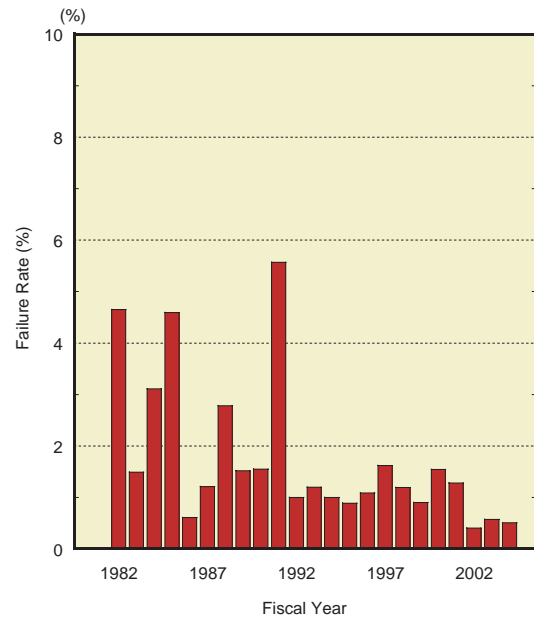


Figure 5 Failure time history.

years. Table 2 gives a breakdown of the causes of unscheduled beam dumps during user time in 2003. The stored beam was lost only ten times in the whole year, with only four beam dumps due to RF system failure. This data demonstrates the high stability and reliability of the accelerator complex, including the RF system which comprises of four 200 kW klystrons and four HOM-damped cavities.

### 3.3 Straight-Sections Upgrade Project of the PF Ring

A major reconstruction of the PF storage ring for the straight-sections upgrade was completed during a seven-month intermission of user experiments in 2005. The main part of this project was the modification of the lattice configuration around the straight sections, keeping intact the orbital polygon itself. As in the emittance upgrade in 1997 for the normal-cell sections, we replaced existing quadrupole magnets with new ones having shorter lengths and higher field gradients, and placed them closer to the neighboring bending magnets. Due to this modification, four new straight sections of 1.4 m (in free space) were produced, and the free space of the existing straight sections was also extended. The upgraded lattice and the extension of the straight sections are illustrated in Fig. 6. The reconstructed area extends over two thirds of the storage ring.

This modification of the lattice configuration alters the physical boundary conditions around the vacuum chambers in the bending magnets and around the beamline frontends. Since the new quadrupole magnets have a different bore diameter from the old ones and have been placed very close to the bending magnets, a number of vacuum chambers including those in the twelve bend sections were replaced with new ones.

The new optics for the upgrade plan is shown in Fig. 7. The creation of new short straight-sections and the extension of two long straight sections are illustrated in Figs. 8 and 10. Following the reconstruction the PF ring will have two 9 m, eight 5 m, and four 1.4 m straight sections as summarized in Table 3. After the upgrade, a total of eleven straight sections will be available for insertion devices. In addition, two short insertion devices can be installed in the two 5.4 m straight sections where the RF cavities are placed. One of these 5.4 m sections will be used exclusively for beam injection.

The dispersion and the beta functions of the straight sections were optimized to be as low as possible. In particular, the vertical beta function of the short straight section was reduced to a minimum of 0.4 m, as shown in Fig. 9. This value is very suitable for a short period undulator. A beam emittance of 27.5 nm rad is expected with the new optics, slightly lower than the present value of 36 nm rad.

Figure 11 shows the section between bending magnets #28 and #01, where a new short straight section was created. The upper image of Fig. 11 shows the

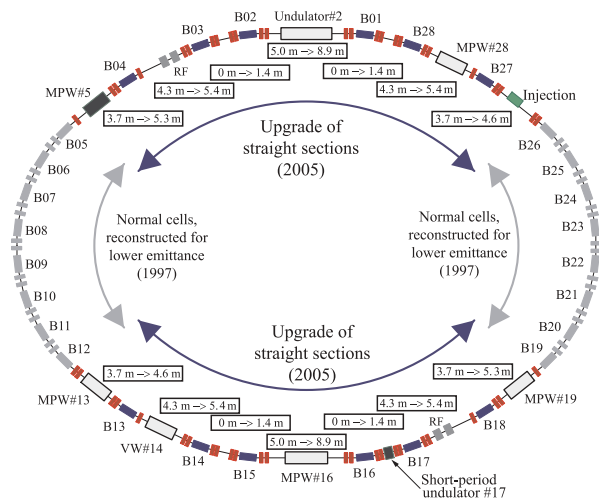


Figure 6 Upgraded lattice and straight-sections area reconstructed for the project.

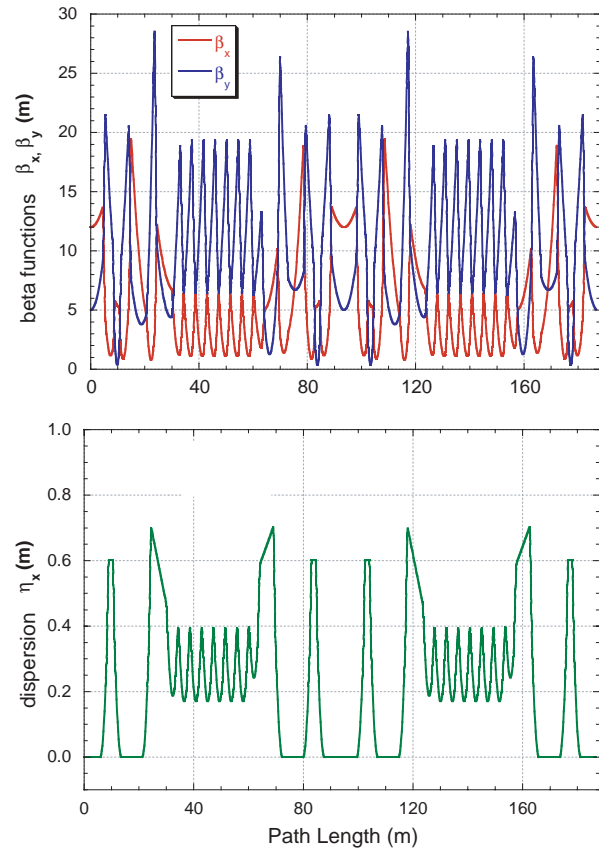


Figure 7 Upgraded optics of the PF storage ring.

previous arrangement, and the lower image shows the new quadrupole arrangement, just before installation of beam ducts. Figure 12 shows the rearrangement of the quadrupoles around MPW#16. Free spaces about 2 m in length were created at either side of MPW#16. Along with the ring reconstruction, the first in-vacuum undulator with a 16-mm period was installed between bending magnets B16 and B17 as a light source for beamline BL-17. Figure 13 shows undulator #17 during installation.

After the reconstruction work was completed in Sep-



Table 3 Extension of the existing straight sections and new short straight sections.

Section	Before Upgrade	After Upgrade	Insertion Devices
B01 – B02	5.0 m	8.9 m	Undulator#02
B15 – B16			Polarization switching U (planning)
B03 – B04	4.3 m	5.4 m	RF cavities
B13 – B14			Super Conducting Wiggler
B17 – B18			RF cavities
B27 – B28			Elliptical U/MPW#28
B04 – B05	3.5 m	5.3 m	MPW#5
B18 – B19			U#19 (revolver)
B12 – B13	4.3 m	5.4 m	U/MPW#13
B26 – B27			injection
B02 – B03	No space	1.4 m	Short Gap Undulator#03 (2006)
B14 – B15		(new)	
B16 – B17			Short Gap Undulator#17 (2005)
B28 – B01			

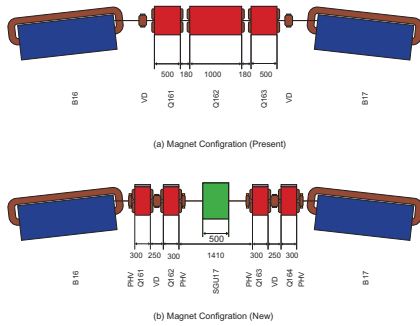


Figure 8 Creation of short straight section.

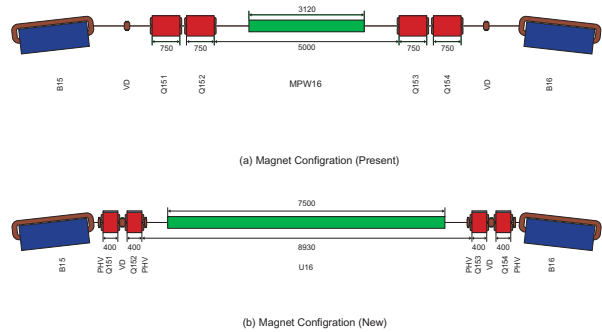


Figure 10 Extension of long straight section.

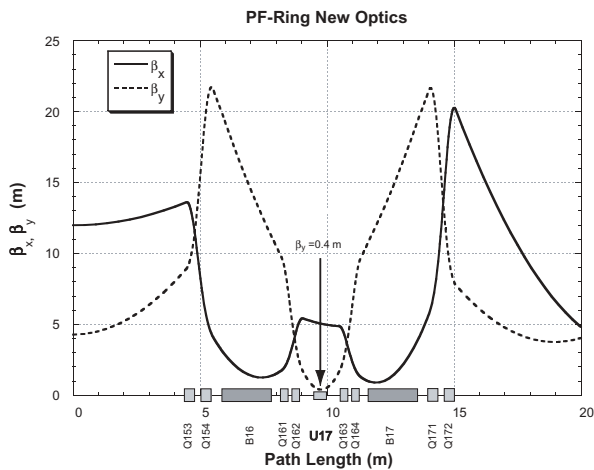


Figure 9 Improvement in optics at the short straight section.

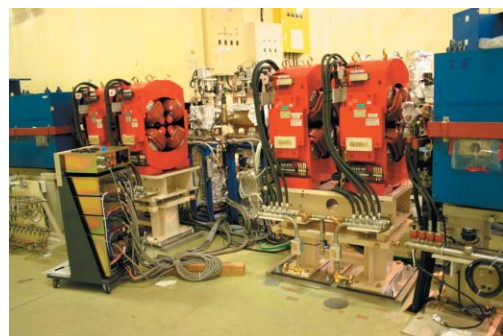


Figure 11 Images before (top) and after (bottom) the rearrangement of the quadrupoles where the short straight section was created.



Figure 12  
Images before (top) and after (bottom) the rearrangement of the quadrupoles around MPW#16. Free spaces of 2 m long were created at either side of MPW#16.



Figure 13  
Short period undulator #17 installed in the ring.

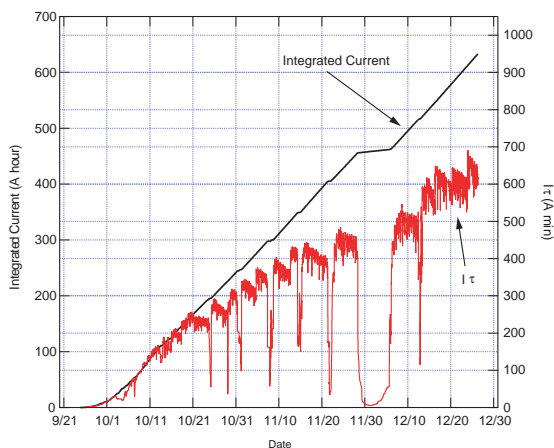


Figure 14  
Growth of integrated current (A hour) and  $I\tau$  (A min) during the 3-months of operation following the straight-sections upgrade.

tember 2005, the storage ring was successfully commissioned and user operation resumed in October 2005. During the commissioning, it was confirmed that a minimum gap of 4 mm for undulator #17 can be achieved without any interference to the stored beam, a value slightly lower than the design value. As user operations continued without any serious trouble, the beam lifetime (or  $I\tau$ ) had already recovered to nearly half of that before the reconstruction by the end of 2005, as shown in Fig. 14. During the first 3-months of operation following the upgrade, the pace of  $I\tau$  recovery has been much faster than what was experienced following the 1997 reconstruction.

### 3.4 Plans for Top-up Operation of the PF Ring : Injector Upgrade Project

The KEK linac is a 600-m long injector for four different storage rings (PF, PF-AR, KEKB e- and e+). The KEKB rings are operated under continuous injection mode (CIM) with 10-Hz repetition rate in order to enhance integrated luminosity, and simultaneous injection of electron and positron beams is planned for the future Super-KEKB project. An up-grade of the linac to perform fast beam mode switching at up to 50-Hz so that each beam pulse can be injected into the PF ring, the PF-AR and the B-factory rings is planned by the injector upgrade committee (IUC). The early discussions of the IUC mainly focused on a fast beam switching system between continuous-injection operation of the B-factory and machine studies which need continuous injection at the PF ring or the PF-AR. Since by using this fast switching system we can use the beam from the linac not only to carry out machine studies but also for daily operation of the PF ring, we started to consider the possibility of top-up injection for the PF ring. We plan to pursue this development in the following three phases.

Phase I. Construct an independent beam transport line in the third switching yard to extract the linac beam independently from the B-factory as shown in Fig. 15. Design common optics for the linac for both PF injection and B-factory injection. Install a pulsed bending magnet instead of a DC switching magnet at the entrance of the beam transport line. After these improvements, we will be able to inject the beam into the PF ring every 20 minutes.

Phase II. Establish the pulse by pulse and multi-energy fast switching system for the linac. After this improvement, we will be able to operate the PF ring with top-up injection during the electron operation mode of the linac.

Phase III. Establish simultaneous acceleration of the electron and the positron beams in the linac. This will enable the PF ring to be operated with full-time top-up injection.

The upgrades necessary for phase I was completed in 2005. A new PF-BT was constructed in the third switching yard so that the BT line makes a detour to avoid the ECS magnets, as shown in Fig. 15. In autumn





### PF-AR User Operation

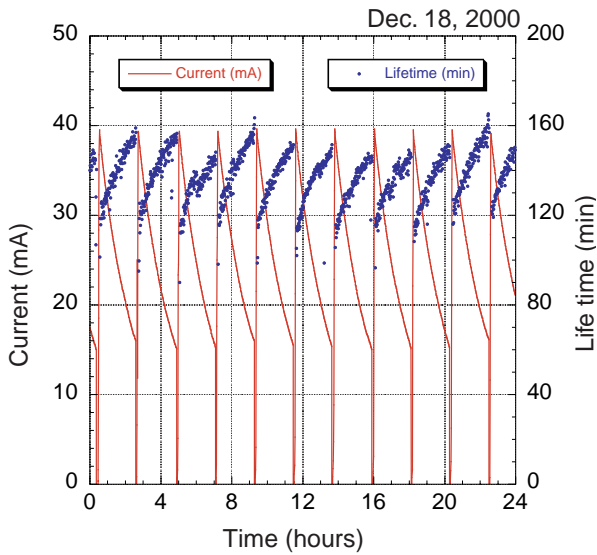


Figure 17  
Typical one-day operation at 6.5 GeV before the upgrade.

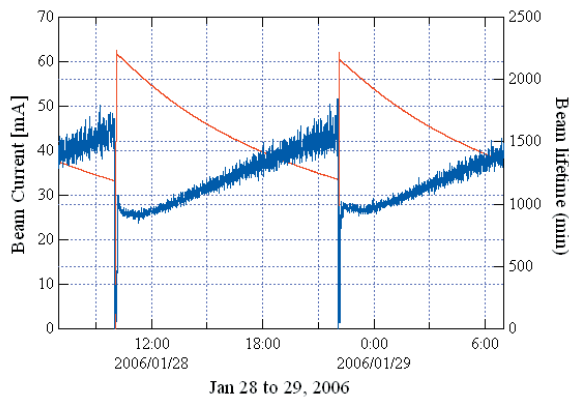


Figure 18  
Present typical one-day operation of the PF-AR at 6.5 GeV.

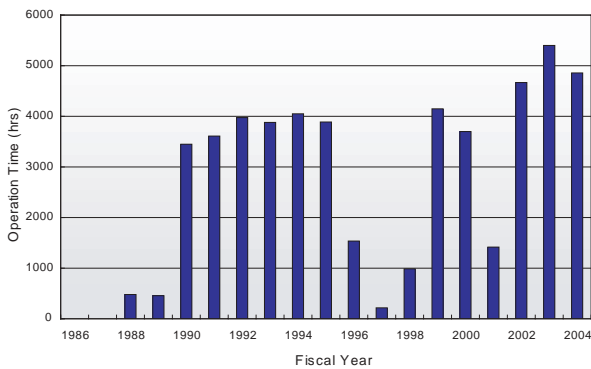


Figure 19  
Operation time history of PF-AR.

Table 4 Operation statistics of PF-AR in FY2004.

Operation Time	4857.0 h	
SR Experiment	3941.5 h	81.2%
Beam Development	733.5 h	15.1%
Failure	98.5 h	2.0%
Miscellaneous	83.5 h	1.7%

vertical beam size can be varied. Also, since single-bunch operation is not a requirement of the medical applications, double-bunch operation can be used in an attempt to increase the beam current and resolve some other issues.

During 5.0 GeV operation, there were several problems to be solved, such as the temperature rise of some vacuum components, a pressure increase in the ring, and a sudden drop in the lifetime. The temperature rise during the 5.0 GeV operation for some vacuum components was considerably greater than during the 6.5 GeV operation, and this was thought to be due to the shortened bunch length at 5.0 GeV. Since November 2003 a new method for avoiding these issues and increasing the beam current has been attempted: double-bunch injection. Since the temperature rise in the vacuum components depends on the beam current per bunch, double-bunch injection is effective in reducing this effect, since the current per bunch can be reduced while maintaining the same total stored current.

In order to achieve double-bunch injection it was necessary to improve the beam feedback system. Without the feedback system the maximum beam current was limited to 10 mA. After modification of the feedback system, a beam current of 70 mA could be stored. The use of double-bunch mode also lowered the temperature of the vacuum components, and the sudden drops in the lifetime were not observed anymore. Figure 20 shows the beam current and beam lifetime for the 5.0

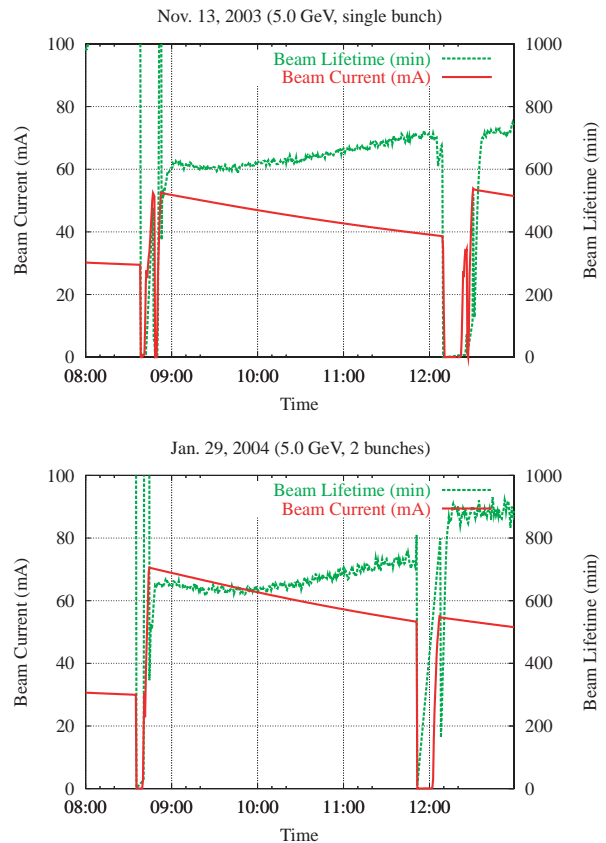


Figure 20  
Beam current and beam lifetime during the medical application for (a) single-bunch and (b) double-bunch operation.



GeV medical applications operation during single-bunch and double-bunch operation.

### 3.6 Development of Insertion Devices

After 2001, the construction of new undulator beamlines has continued in the new experimental hall of the PF-AR and in the upgraded straight sections of the PF ring. The specifications of the newly developed undulators are summarized in Table 5. All undulators for the PF-AR have been constructed as hard X-ray sources using the in-vacuum configuration, and two of them have a tapering mechanism to produce a wide bandwidth spectrum. The first in-vacuum type undulator of the PF ring was installed into one of the new short straight sections in 2005. This undulator has a particularly short magnetic period and a narrow minimum gap to produce hard X-rays up to 15 keV even with 2.5 GeV electron energy. The development of short period magnetic arrays has continued for the next in-vacuum undulators of the PF ring. Design of a fast polarization switching undulator which takes advantage of the extended straight section of the PF ring is under way.

#### **U#NW2 and U#NW12, Tapered Undulators**

In 2001 and 2002, we installed two in-vacuum type undulators with tilt mechanisms on the magnet arrays (U#NW2 and U#NW12) at the PF-AR. The tilt mechanism was devised and developed to satisfy two user requirements. One of these requirements was for a very sharp spectrum that is suitable for ordinary diffraction experiments in the hard X-ray region, the other was for a relatively wide spectrum (relative bandwidth of 10s of percent) for example for XAFS experiments. In the construction of these undulators, we employed pure Halbach type magnet arrangements with a period length of 4 cm and period numbers of 90 (for U#NW2) and 95 (U#NW12). The selection of the period length

was made to cover the photon energy region from 5 keV to 25 keV with the higher harmonics (up to 5th) with the 6.5 GeV operation of the PF-AR. A taper of up to  $\pm 2$  mm was allowed for mechanically in the present construction in terms of the difference in the gap size at the entrance and at the exit of the undulator. Calculated spectra corresponding to the tapered mode are given in Fig. 21. The calculation was made on the measured undulator field by direct Fourier transformation with the parameters given in Fig. 21.

The surfaces of the magnets, made of a porous material (NdFeB), were sealed by a TiN coating. The vacuum chamber (of 200 liters capacity) which contains the magnet arrays was evacuated down to  $1 \times 10^{-8}$  Pa using nonevaporable getter (NEG) pumps (4000 l/s for U#NW2 and 5000 l/s U#NW12) and sputter ion pumps (240 l/s for U#NW2 and 480 l/s U#NW12) following vacuum bakeout at 120°C. In order to avoid high-temperature deterioration of the magnets during the bake-out process, the magnets were pre-baked at 145°C following magnetization.

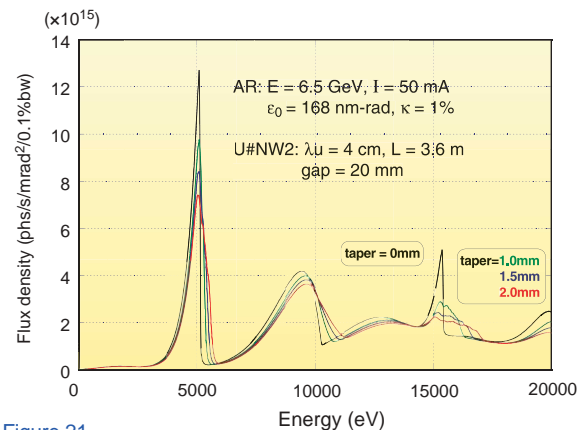


Figure 21  
Calculated spectra for the tapered mode are compared to that for the ordinary mode. The calculation is made on the basis of the measured magnetic field.

Table 5 Chronological table of the development of new undulators.

Year	Beamline	period	Notes
2001	AR-NW2	40 mm, N=90	in vacuum, wide bandwidth by tapering, 5-25 keV
2002	AR-NW12	40 mm, N=95	in vacuum, wide bandwidth by tapering, 5-25 keV
2003	PF-BL05	60 mm, N=5	Test for polarization switching at 1 Hz
2003	PF-BL05	120 mm, N=21	Multi Pole Wiggler, 10-15 keV
2005	PF-BL17	16 mm, N=29	narrow gap 4 mm, in vacuum, 15 keV
2005	AR-NW14	36 mm, N=80	in vacuum, 5-25 keV
2006	PF-BL03	18 mm, N=26	narrow gap 4 mm, in vacuum, 15 keV
2006	AR-NW14	20 mm, N=75	in vacuum, 13-18 keV
2007	PF-BL16	60 mm, N=58	Tandem, polarization switching at 10 Hz, 0.25-1.5 keV

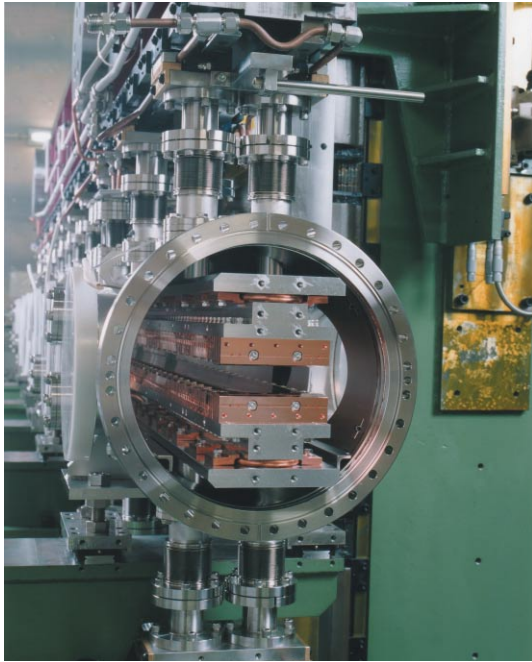


Figure 22  
Inside view of the in-vacuum undulator, U#NW2.

### Multipole Wiggler #05

In 2003, we installed a multipole wiggler (MPW#05) in the straight section between bending magnets #04 and #05 of the PF ring. MPW#05 is used exclusively as a light source for protein crystallography. For this purpose, the required energy region of the synchrotron radiation is mainly 10 keV to 15 keV. In the design stage, we tried to optimize the parameters of MPW#05 so that the photon flux density would be as high as possible in this energy region and the magnetic attractive force between the magnet arrays minimized without degradation of the field quality. Under the constraints of the proposed accelerator design for the straight-sections upgrade, we found that a combination of a period length of 12 cm and a periodicity of 21 would be most suitable for the available length between bending magnets #04 and #05, as shown in Fig. 23. In order to achieve the required field intensity of 1.4 T at a magnet gap of 26 mm, we adopted a hybrid magnet arrangement: NdFeB is used for the permanent magnet, and vanadium-Permendur for the iron core. The maximum K value is 15.8 at the minimum gap of 26 mm. Calculated spectra of the synchrotron radiation from MPW#05 are shown in Fig. 24. The spectra for the undulator radiation (up to the 7th harmonic) are also shown along with that for the wiggler radiation. The measurement and the adjustment of the magnetic field were performed using a 2-dimensional Hall probe system and a flipping coil system.

### Very Short Period Undulator (SGU#17) for the New Straight Section of the PF ring

Four new 1.4 m straight sections have been created in the straight-sections upgrade project. These straight sections were designed to have small betatron functions so that in-vacuum type undulators with very short magnetic periods and gaps could be installed. Over the

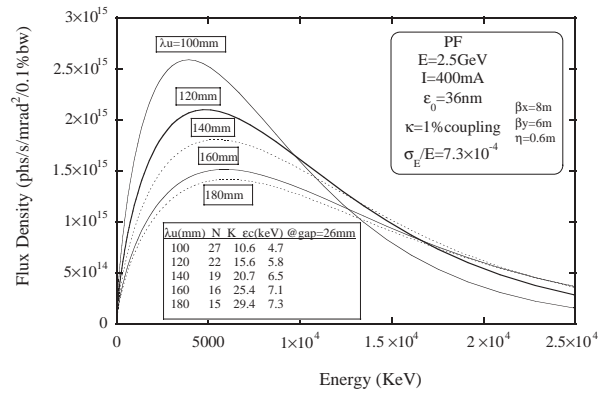


Figure 23  
Comparison of the calculated photon flux densities with several period lengths. Total length of the magnet array is kept constant.

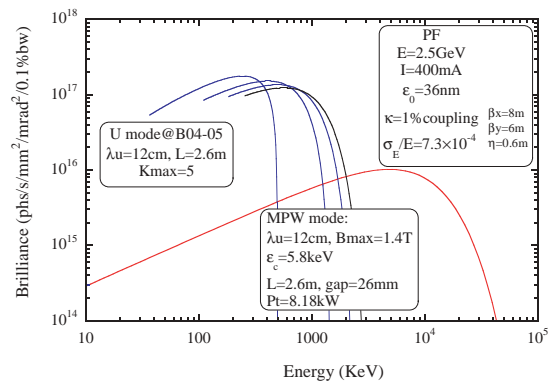


Figure 24  
Spectral properties of MPW#05 in the PF ring. In addition to a wiggler mode, the spectra in the case of an undulator mode are shown.

past few years, we have been developing short-period undulator magnets, and in 2004 we installed a short-period, short-gap in-vacuum undulator (SGU) at the 2.5 GeV PF storage ring as a hard X-ray source for protein crystallography. Even with the 2.5 GeV electron energy of the PF ring, it is possible to produce hard X-rays up to 15 keV by selecting a very short undulator period length, as shown by the spectra of Fig. 25. However, these spectra are only valid when the undulator can be set to a very short gap, of the order of 5 mm or less. This can be accomplished by a combination of in-vacuum undulator technology and an advanced lattice design with small betatron functions. The completed in-vacuum undulator (SGU#17) was installed in the straight section between bending magnets B#16 and B#17 in the upgraded PF lattice. The vertical betatron function was designed to be 0.4 m at the center of this section, allowing a minimum gap of 4.5 mm for SGU#17.

The new undulator employs a pure Halbach-type magnet arrangement with a period length ( $\lambda_u$ ) of 16 mm in order to obtain photon energies of up to 15 keV from the lower (1st to 7th) harmonics of the undulator radiation. Due to the limited length available at the installation site we have adopted a periodicity (N) of 29. For the magnet material we have selected an Nd-Fe-B alloy with a remnant field of  $B_r=12.0$  kG and a coercivity of  $iH_c=28$  kOe (NEOMAX35VH manufactured by NEOMAX Co.

Ltd.), providing excellent magnetic performance and endurance against the high temperatures applied during baking. Magnet blocks made from this porous alloy are coated with a 5  $\mu\text{m}$  layer of TiN for vacuum sealing, embedded in a holder made of oxygen-free copper, and attached to a pair of aluminium magnet-mounting beams. The magnet system components are enclosed in a stainless steel vacuum chamber with an electrolytically polished internal surface. The size of the chamber is 250 mm (inner diameter)  $\times$  980 mm. The magnet gap can be varied from 40 mm to 4.5 mm (with a deflection parameter  $K$  ranging up to 1.27), and is controlled by a translation system composed of precise ball screws and linear guides. In order to avoid problems due to Ohmic and parasitic mode losses, we have covered the opposing faces of the magnet arrays with a thin metal foil made of oxygen-free copper (60  $\mu\text{m}$ ) plated with Ni (25  $\mu\text{m}$ ) for magnetic sustainment. The end of the magnet array is also connected to the Q-duct of the PF ring using a flexible 180  $\mu\text{m}$  Be-Cu foil. Field adjustments were made on the basis of precise field measurements using Hall probes oriented in the x- and y-directions, as shown in Fig. 26. We adjusted the undulator field by optimizing the kick angle of the electrons at each pole to produce an ideal sinusoidal orbit in the horizontal plane and also to have a straight orbit in the vertical plane. Figure 27 shows the radiation spectrum for SGU#17 at a gap of 5.4

mm ( $K=1.05$ ). The calculation was made using the 2.5 GeV PF ring parameters given in the inset to the figure.

### Two New In-Vacuum Undulators for AR-NW14

During the past few years, the non-equilibrium dynamics project has been underway at the 6.5 GeV PF-AR. To support this project, we have modified the RF sections of the PF-AR to create empty straight sections for insertion devices, and have constructed a new beamline BL#NW14. Two of the four RF cavities in the west RF section were moved to the east section, where there were already two cavities in operation (see Fig. 28). In the new straight sections we plan to install two new in-vacuum type x-ray undulators (U#NW14-36 and U#NW14-20) in the furthest downstream section and the neighbouring section for beamline BL#NW14.

In the construction of these undulators, we have employed the same in-vacuum technology used already for several of the PF-AR undulators, and adopted a pure Halbach type magnet arrangement with period lengths  $\lambda_u=36$  mm for U#NW14-36 and  $\lambda_u=20$  mm for U#NW14-20. The numbers of periods were chosen to be  $N=80$  for U#NW14-36 and  $N=75$  for U#NW14-20. For U#NW14-36 the period length was chosen to cover the photon energy region of 5-25 keV under 6.5 GeV operation using up to the fifth-order harmonics (see Fig. 29.) For U#NW14-20 the period length was chosen for the first harmonic to cover the energy region of 13-18 keV under the same conditions. Figure 30 shows how the spectrum from U#NW14-20 depends on the magnet gap.

For the magnet material we have selected an Nd-Fe-B alloy with a remnant field of  $B_r=12.0$  kG and a coercivity of  $iH_c=28$  kOe (NEOMAX35VH, NEOMAX Co. Ltd.) for its excellent magnetic performance and endurance against the high temperatures reached during baking. Magnet blocks made of the porous alloy were coated with a 5- $\mu\text{m}$  layer of TiN to create a vacuum-tight seal, embedded in an oxygen-free copper holder, and attached to a pair of aluminium magnet-mounting beams. Magnetic measurements and adjustments for U#NW14-36 have been completed, and installation in the PF-AR was carried out during summer 2005. The

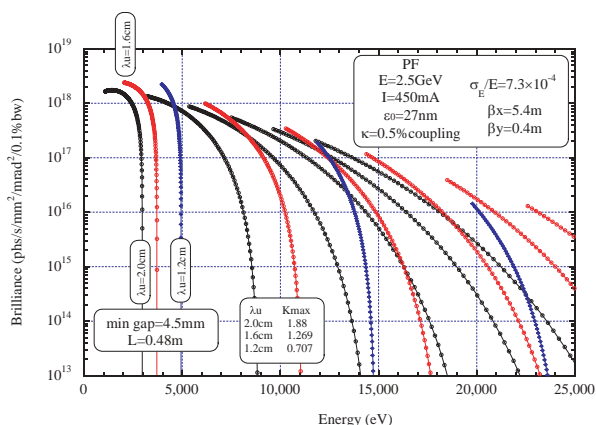


Figure 25  
Example spectra of an SGU radiation.

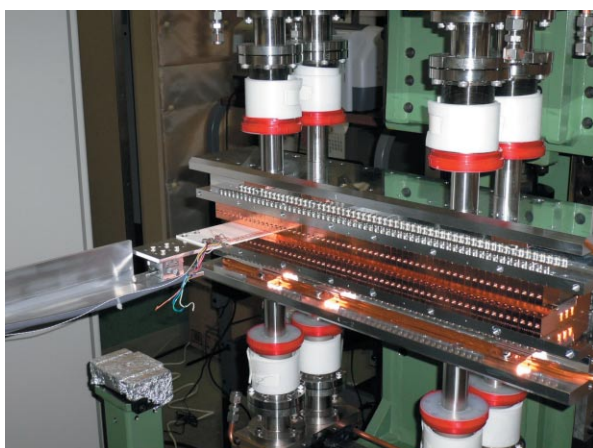


Figure 26  
Photograph of an SGU during magnetic measurements.

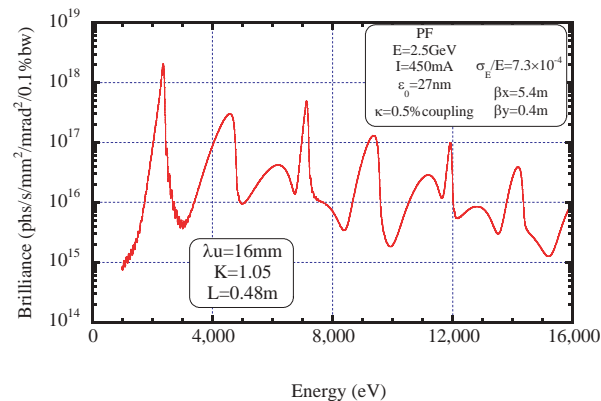


Figure 27  
Calculated spectrum of the SGU with  $\lambda_u=16$  mm at  $K=1.05$ .

installation and commissioning of U#NW14-20 will be carried out in 2006.

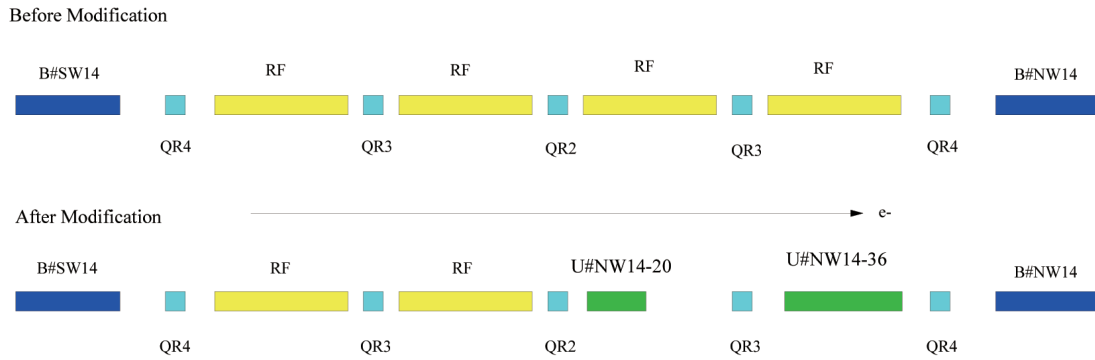


Figure 28  
Modification of the west RF section in the PF-AR.

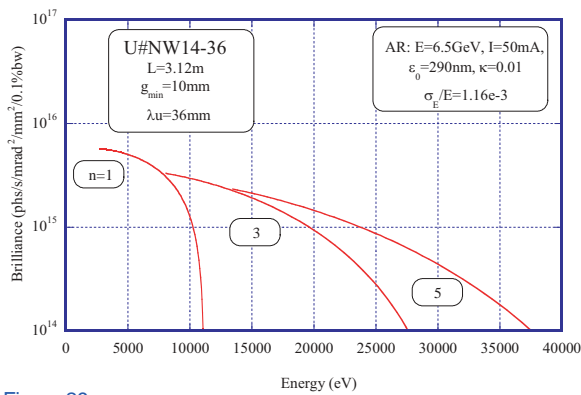


Figure 29  
Spectra of the radiation from U#NW14-36. Brilliance of the first, third and fifth harmonics are shown.

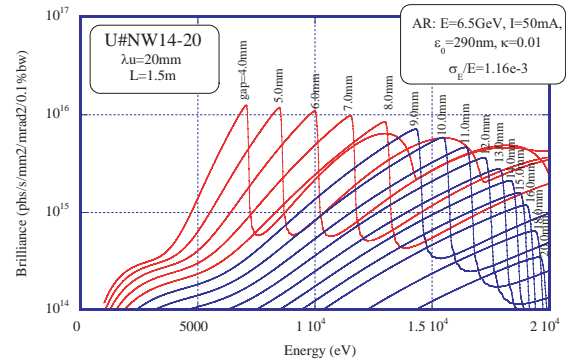


Figure 30  
Spectra of the radiation from U#NW14-20. The first harmonic covers an energy region from 13 to 18 keV as the magnet gap is changed from 8 mm to 14 mm.